2011 American Control Conference
on O'Farrell Street, San Francisco, CA, USA
June 29 - July 01, 2011

PDE Model for Thermal Dynamics of a Large Li-Ion Battery Pack

Andrey Smyshlyaev, Miroslav Krstic, Nalin Chaturvedi, Jasim Ahmed, and Aleksandar Kojic

Abstract— **Technologies for storage of electric energy are central to a range of applications—from transportation systems, including electric and hybrid vehicles, to portable electronics. Lithium-ion batteries have emerged as the most promising technology for such applications, thanks to their high energy density, lack of hysteresis, and low self-discharge currents. One of the most important problems in battery technology is achieving safe and reliable operation at low cost. Large packs of batteries, required in high-power applications such as submarines, satellites, and electric automobiles, are prone to thermal runaways which can result in damage on a large scale. Safety is typically ensured by over-design, which amounts to packaging and passive cooling techniques designed for worst-case scenarios.**

Both the weight and the cost of the batteries can be considerably lowered by developing models of thermal dynamics in battery packs and model-based estimators and control laws. At present, only detailed numerically-oriented models (often referred to as CFD or FEM models) exist, which are used for computationally intensive off-line tests of operating scenarios, but are unsuitable for real-time implementation.

In this paper, we develop a model of the thermal dynamics in large battery packs in the form of two-dimensional partial differential equations (2D PDEs). The model is a considerable simplification of the full CFD/FEM model and therefore offers the advantage of being tractable for model-based state estimation, parameter estimation, and control design.

The simulations show that our model matches the CFD model reasonably well while taking much less time to compute, which shows the viability of our approach.

I. Introduction

Technologies for storage of electric energy are central to a range of applications—from transportation systems, including electric and hybrid vehicles, to portable electronics. Lithium-ion batteries have emerged as the most promising technology for such applications, thanks to their high energy density, lack of hysteresis, and low self-discharge currents [1], [2].

Electric automobiles and submarines demand large amounts of energy and power, and therefore need packs of thousands of Li-ion cells (for example, the battery pack in the Tesla Roadster car has 6,800 cells [5]). One of the challenges in dealing with battery packs is that after a period of usage, the state of health of individual cells is highly non-uniform due to electrical and thermal interactions of the individual cells. Charging all the cells to their full capacity becomes unachievable because it would lead to some of the cells exceeding the maximum voltage, above which they become thermally unstable. Even when a battery pack is not in use, namely, neither being charged nor discharged, a reasonable probability exists that, in an aging, or inexpensively produced battery pack, one of the many cells in a pack undergoes short circuit. This results in the cell overheating and igniting. The high temperature produced by such a cell leads to electrical and thermal transients in the neighboring cells which results in a chain reaction where an entire pack explodes. This phenomenon is called thermal runaway (Fig. 1).

While thermal runaways in battery cells in portable computers have been widely publicized [6], the danger from them is limited. Thermal runaway in large battery packs can result in damage on a large scale. An illustrative example is a recent accident [7] described in [8], with the US Navy's new 65-foot mini-submarine named Advanced SEAL Delivery System (ASDS). The ASDS is designed to carry a team of about ten special operations forces and, for stealth reasons, is propelled by an electric motor, which is powered by a Li-ion battery pack. In November 2008, the battery pack in an ASDS stationed in Pearl City, Hawaii, underwent a thermal runaway while recharging in its home port. While no one was hurt, the fire took several hours to put out and the repair cost is estimated at $237 million.

Safety is typically ensured by over-design, which amounts to packaging and passive cooling techniques designed for worst-case scenarios. For example, in some battery designs, such as for the Tesla Roadster car [5], liquid cooling lines are incorporated, with a 50/50 mixture of water and glycol. The safety-driven over-design adds not only to the weight but also to the cost of the batteries. For example, the replacement price of the battery pack in the Tesla Roadster car is $36,000 and not anticipated to fall below $10,000 before 2017. Better understanding of the thermal dynamics in battery packs, state estimation to spatially locate the "hot spots" in the pack using temperature sensor at only a limited number of locations in the pack, and more intelligent control systems that employ parameter estimators of the uncertain thermal conductivity within and in-between cells, are crucial for developing cheaper batteries that will enable commercialization of the environmentally-friendly electric and plug-in hybrid vehicles.

At present, only detailed numerically-oriented models (often referred to as CFD or FEM models) exist [4], [3], which are used for computationally intensive off-line tests of operating scenarios, but are unsuitable for real-time implementation. Since the computational burden of these models is prohibitive, other, sufficiently detailed but computationally

This work was supported by NSF.

Andrey Smyshlyaev and Miroslav Krstic are with the Department of Mechanical and Aerospace Engineering, University of California, San Diego, La Jolla, CA 92093-0411 USA (e-mail: krstic@ucsd.edu, asmyshly@ucsd.edu).

Nalin Chaturvedi, Jasim Ahmed, and Aleksandar Kojic are with Robert Bosch LLC, Research and Technology Center, Palo Alto, California.

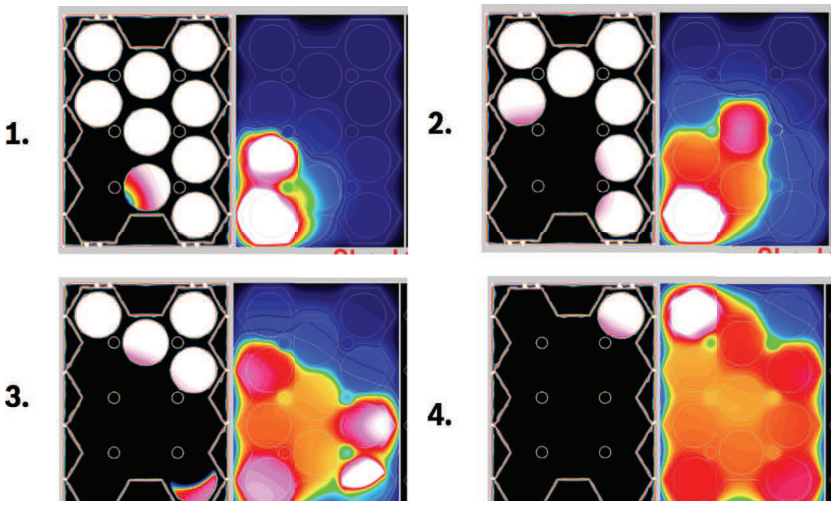

Fig. 1. An illustration of thermal runaway in a battery pack. It starts in snapshot 1 with the cell in the lower left corner drawing high current and overheating, progressing through snapshots 2 and 3 to 4, where the entire pack is ignited.

tractable models and estimators are needed. In this paper we make the first step in developing such models. Our models emphasize the inhomogeneity of the battery pack medium, where, the cells and the materials they are enclosed in have very different thermal conductivity properties, where the thermal dynamics are coupled with the electrical dynamics which act as heat sources, and where cooling systems—passive or controlled—may be introduced to manage the temperature distribution in a battery pack. These models are in the form of partial differential equations and capture the spatially distributed character of the thermal dynamics in a pack. Being a considerable simplification of the full CFD/FEM model, they offer the advantage of being tractable for model-based state estimation, parameter estimation, and control design [10], [11].

II. A Reduced CFD Model of Thermal Dynamics in a Battery Pack

Since the CFD data is available only for small packs of dozen batteries, as a first step, we develop a "reduced" CFD model, which consists of finite-dimensional models of individual cells and cooling pipes and a CFD model of the pack material. The reduced model will allow us to indirectly compare the PDE model (developed in the subsequent sections) with the CFD model on large battery packs.

Battery cells are typically cylindrical in shape and in battery packs they are arranged in arrays, such as shown in Figure 2. The thermal dynamics in a cell, as well as in a battery pack, are three-dimensional. However, relatively little transient occurs in the direction parallel to the axes of the cells as compared to the plane perpendicular to the axes. Hence, we put emphasis on the 2D dynamics in the radial direction of the battery cells in a pack (shown in Figure 1).

Consider the 2D battery pack shown in Figure 3. Our goal is to develop a simplified model of thermal dynamics that works for packs of any size and matches CFD data reasonably well.

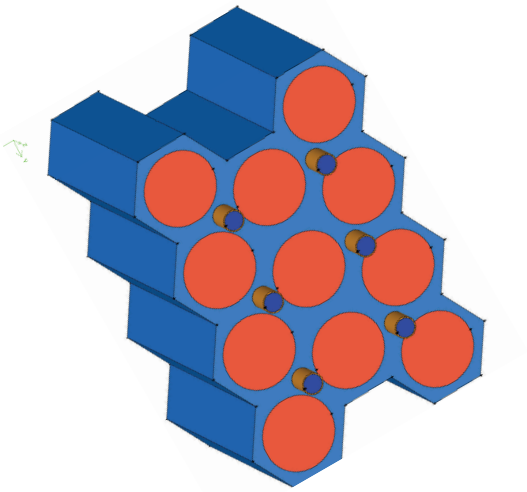

Fig. 2. A battery pack with coolant lines.

We are going to separately model the thermal dynamics in the cells, in the cooling pipes, and in the pack material. For the thermal model of the pack material we use the basic heat equation

$$\rho_{\mathrm{p}} c_{\mathrm{p}} \frac{\partial \Theta}{\partial t} = k_{\mathrm{p}} \nabla \Theta, \qquad (x, y) \in \Omega\,, \tag{1}$$

where ρ_{p}, c_{p}, and k_{p} are, respectively, the density, the specific heat, and the thermal conductivity of the pack material, $\Theta(x, y, t)$ is the temperature of the pack material, and Ω is the domain occupied by the pack material.

Let us denote the temperatures of the cells by $T_i(t)$, $i = 1, \ldots, N_c$ (N_c is the number of cells) and the temperatures of the cooling pipes by $T_{w,j}(t)$, $j = 1, \ldots, N_p$ (N_p is the number of pipes).

At the outside boundary of the pack we have the following boundary condition:

$$k_{\mathrm{p}}(\mathbf{n} \cdot \nabla \Theta) = h_{\mathrm{pa}}(T_{\mathrm{air}} - \Theta), \quad (x, y) \in \Gamma, \tag{2}$$

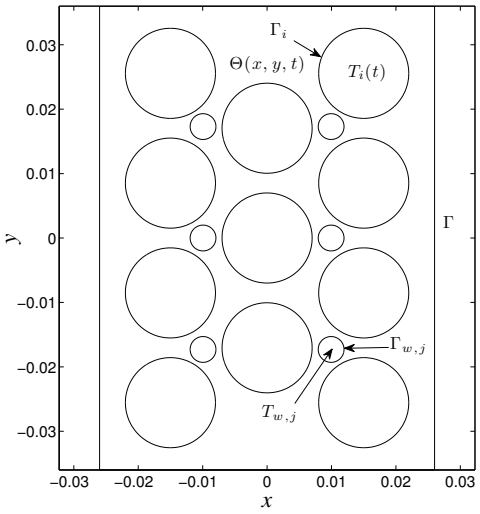

Fig. 3. 2D battery pack.

where $T_{\rm air}$ is the temperature of the air and $h_{\rm pa}$ is the heat transfer coefficient between the pack and outside air.

The boundary conditions at the cell boundaries are

$$k_{\rm p}(\mathbf{n}\cdot\nabla\Theta) = h_{\rm pc}(T_i - \Theta), \quad (x,y)\in\Gamma_i \tag{3}$$

for $i = 1,\dots,N_c$, and the boundary conditions at the pipe boundaries are

$$k_{\rm p}(\mathbf{n}\cdot\nabla\Theta) = h_{\rm pw}(T_{w,j} - \Theta), \quad (x,y)\in\Gamma_{w,j} \tag{4}$$

for $j = 1,\dots,N_p$, where $h_{\rm pc}$ is the heat transfer coefficient between the pack material and cells and $h_{\rm pw}$ is the heat transfer coefficient between the pack material and cooling pipes.

Using basic laws of heat transfer, we get the following ODE models for the cells:

$$\dot{T}_i = \frac{h_{\rm pc}}{\rho_{\rm c}c_{\rm c}\pi r^2}\int\limits_{\Gamma_i}(\Theta - T_i)\,d\Gamma_i + \frac{1}{\rho_{\rm c}c_{\rm c}}\Pi_i \tag{5}$$

for $i = 1,\dots,N_c$. Here, $\Pi_i(t)$ is the current-driven heating of the cell i, $\rho_{\rm c}$ is the density of the cell and $c_{\rm c}$ is the specific heat of the cell material. The term $\Pi_i(t)$ has a complicated structure (it couples electric and thermal dynamics of the cells), but for the purpose of developing a useful thermal model we assume that it can be measured/estimated.

The models for the cooling pipes are

$$\dot{T}_{w,j} = \frac{h_{\rm pw}}{\rho_{\rm w}c_{\rm w}\pi r_p^2}\int\limits_{\Gamma_{w,j}}(\Theta - T_{w,j})\,d\Gamma_{w,j} - \frac{\dot{m}_{\rm w}(T_{out,j} - T_{in})}{\rho_{\rm w}\pi r_p^2 L}$$

for $j = 1,\dots,N_p$, where $\rho_{\rm w}$, $c_{\rm w}$ are the density and the specific heat of the coolant, r_p is the radius of the pipe, $\dot{m}_{\rm w}$ is the coolant flow rate, L is the length of the pipe in the direction of the axes of the cells, and T_{in} and $T_{out,j}$ are the temperatures at the inlet and the outlet of the pipe, respectively.

The reduced model simplifies the full CFD model in several ways. First, it is a 2D model as opposed to 3D CFD model. Second, it uses scalar rather than distributed states to describe temperature evolution of the cells. Also, electric-thermal coupling is neglected.

The results of numerical comparison of the reduced model and the full CFD model are presented in Figures 4–6. The initial temperature of the pack is 295K, and the cells are heated at the rate $\Pi_i(t) = 10^7{\rm W/m}^3$ for 20 seconds at which point the heat generation is turned off. The PDE part of the model was computed using the finite element method. We can see that the reduced model is in a good agreement with the CFD model.

III. PDE Model of a Large Battery Pack

Although the model obtained in the previous section is considerably simpler than the CFD model, it is still not suitable for large battery packs. Our objective now is to further simplify the reduced model to obtain a model that is tractable for control design and state and parameter estimation when the pack is of a very large size.

To derive this model, we start by partitioning the pack into the triangular and hexagonal elements, as shown in Figure 7. Note that we rearranged the cooling pipes so that they are more evenly distributed in a large pack.

The round cells are approximated by hexagons that have an area equal to the area of the cells and the pack material between the cells is divided into (truncated) triangular elements. Given the length of the edge of a hexagon cell (l) and the horizontal distance between the cells (Δx), we can compute the following parameters:

$$l = r\frac{\sqrt{2\pi}}{\sqrt{3\sqrt{3}}}, \quad a = \frac{2}{3}\Delta x, \quad S = \frac{\Delta x^2}{\sqrt{3}} - \frac{3\sqrt{3}}{4}l^2, \tag{6}$$

where r is the radius of a cell, a is the distance between the centers of any two adjacent elements, and S is the area of the triangular elements.

There are two types of pack elements: with and without cooling pipes. The laws of heat transfer lead to the following equations (see the index notation in Fig. 7):

$$\begin{aligned}\dot{\Theta}_{i+\frac{1}{3},j+1} &= \alpha_1\left(T_{i,j} + T_{i,j+2} + T_{i+1,j+1} - 3\Theta_{i+\frac{1}{3},j+1}\right)\\ &+ \beta_1\left(\Theta_{i+\frac{2}{3},j+2} + \Theta_{i+\frac{2}{3},j} + \Theta_{i-\frac{1}{3},j+1} - 3\Theta_{i+\frac{1}{3},j+1}\right)\end{aligned} \tag{7}$$

for the pack elements without the cooling pipes and

$$\begin{aligned}\dot{\Theta}_{i+\frac{2}{3},j} &= \alpha_2\left(T_{i,j} + T_{i+1,j+1} + T_{i+1,j-1} - 3\Theta_{i+\frac{2}{3},j}\right)\\ &+ \beta_2\left(\Theta_{i+\frac{1}{3},j+1} + \Theta_{i+\frac{1}{3},j-1} + \Theta_{i+\frac{4}{3},j} - 3\Theta_{i+\frac{2}{3},j}\right)\\ &+ \gamma_1\left(T_{w,i+\frac{2}{3},j} - \Theta_{i+\frac{2}{3},j}\right)\end{aligned} \tag{8}$$

for the pack elements with the pipes. Here,

$$\alpha_1 = \frac{h_1 l}{\rho_{\rm p}c_{\rm p}S},\ \alpha_2 = \frac{h_2 l}{\rho_{\rm p}c_{\rm p}(S - \pi r_{po}^2)},\ \beta_2 = \frac{\beta_1 S}{S - \pi r_{po}^2} \tag{9}$$

$$\beta_1 = \frac{h_3(\sqrt{3}\Delta x - 3l)}{\rho_{\rm p}c_{\rm p}S}, \quad \gamma_1 = \frac{2h_4\pi r_{po}}{\rho_{\rm p}c_{\rm p}(S - \pi r_{po}^2)}, \tag{10}$$

where h_2, h_1 are the heat transfer coefficients between the cells and the triangular elements with/without pipes, respectively; h_3 is the heat transfer coefficient between the two types of triangular elements; h_4 is the heat transfer

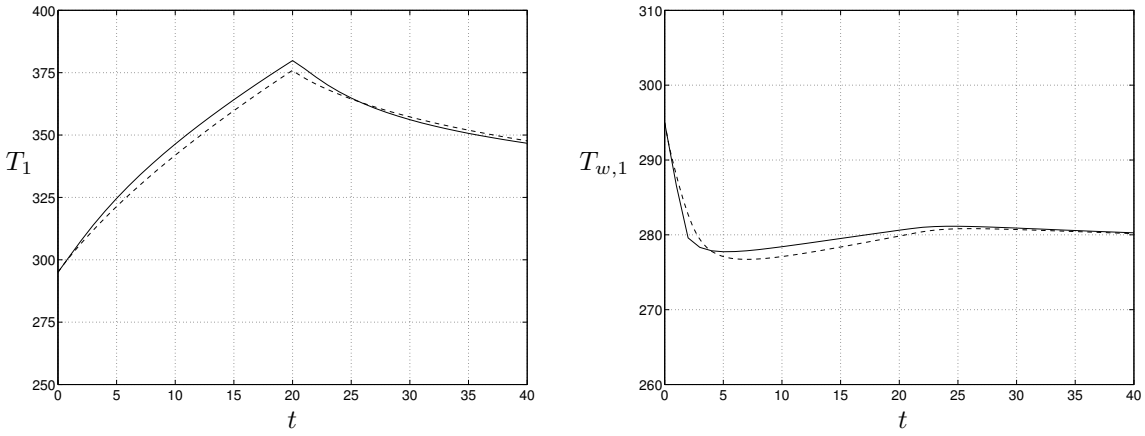

Fig. 4. Left: Evolution of the temperature of the lower left cell (CFD—solid, reduced—dashed). Right: Evolution of the temperature of the lower left pipe (CFD—solid, reduced—dashed).

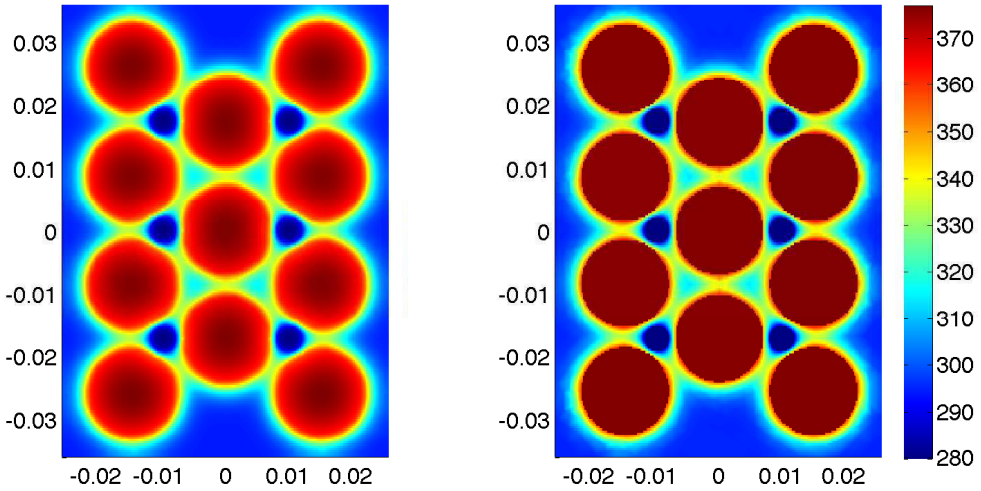

Fig. 5. Temperature distribution in 3x4 battery pack at $t = 20$ seconds. Left: Full CFD model. Right: Reduced model.

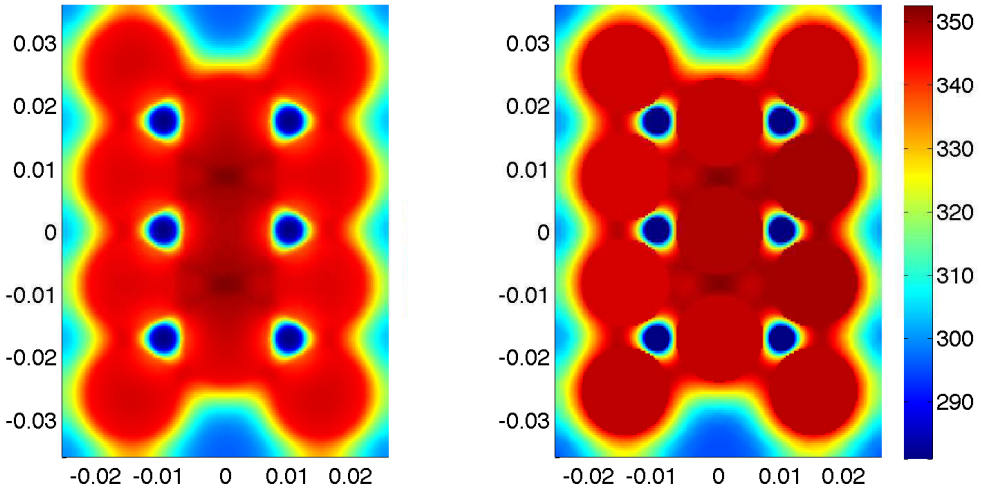

Fig. 6. Temperature distribution in 3x4 battery pack at $t = 40$ seconds. Left: Full CFD model. Right: Reduced model.

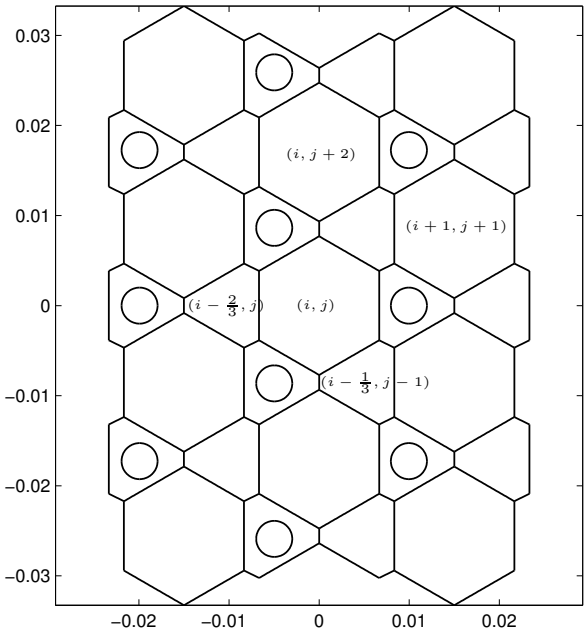

Fig. 7. Partition of the battery pack for the PDE model derivation.

coefficient between the pack material and the coolant, and r_{po} is the outer radius of the cooling pipe.

The heat transfer equations for the cells take the form

$$\dot{T}_{i,j} = \alpha_3 \left(\Theta_{i-\frac{2}{3},j} + \Theta_{i+\frac{1}{3},j+1} + \Theta_{i+\frac{1}{3},j-1} - 3T_{i,j}\right) \quad (11)$$
$$+ \alpha_4 \left(\Theta_{i-\frac{1}{3},j+1} + \Theta_{i-\frac{1}{3},j-1} + \Theta_{i+\frac{2}{3},j} - 3T_{i,j}\right) + \frac{\Pi_{i,j}}{\rho_{\rm c} c_{\rm c}}\,.$$

Here the constants α_3, α_4 are defined as follows:

$$\alpha_3 = \alpha_1 \frac{\rho_{\rm p} c_{\rm p} S}{\rho_{\rm c} c_{\rm c} \pi r^2}, \qquad \alpha_4 = \alpha_2 \frac{\rho_{\rm p} c_{\rm p} (S - \pi r_{po}^2)}{\rho_{\rm c} c_{\rm c} \pi r^2}\,. \quad (12)$$

Finally, the ODE model for the coolant is

$$\dot{T}_{w,i+\frac{2}{3},j} = \gamma_2 \left(\Theta_{i+\frac{2}{3},j} - T_{w,i+\frac{2}{3},j}\right) - \frac{1}{\rho_{\rm w} c_{\rm w}} Q, \quad (13)$$

where

$$Q = \frac{\dot{m}_{\rm w} c_{\rm w} (T_{out}(t) - T_{in}(t))}{\pi r_p^2 L}, \quad \gamma_2 = \gamma_1 \frac{\rho_{\rm p} c_{\rm p} (S - \pi r_{po}^2)}{\rho_{\rm w} c_{\rm w} \pi r_p^2}.$$

To put the equations into the form in which we can pass to the limit of a large number of cells, we use the following approximation for the triangular grid of the size a:

$$\nabla^2 \Theta_{i,j} = \frac{2}{3a^2} \left(\Theta_{i+\frac{1}{3},j+1} + \Theta_{i-\frac{1}{3},j+1} + \Theta_{i+\frac{2}{3},j} + \Theta_{i-\frac{2}{3},j}\right.$$
$$\left. + \Theta_{i+\frac{1}{3},j-1} + \Theta_{i-\frac{1}{3},j-1} - 6\Theta_{i,j}\right) + O(a^2). \quad (14)$$

Composing the sum on the right hand side of (14) using the equations (7) and (8), after tedious but straightforward algebra, we obtain the following set of equations:

$$\dot{\Theta}_{i,j} = \frac{3(\beta_1 + \beta_2) a^2}{8} \nabla^2 \Theta_{i,j} + \frac{3}{2} (\alpha_1 + \alpha_2) (T_{i,j} - \Theta_{i,j})$$
$$+ \frac{\gamma_1}{2} (T_{w,i,j} - \Theta_{i,j})\,, \quad (15)$$

$$\dot{T}_{i,j} = 3(\alpha_3 + \alpha_4)(\Theta_{i,j} - T_{i,j}) + \frac{1}{\rho_{\rm c} c_{\rm c}} \Pi_{i,j}\,. \quad (16)$$

Taking the limit $a \to 0$ (which corresponds to a large number of cells in the pack), we obtain the PDE model

$$\frac{\partial \Theta}{\partial t} = kR \nabla^2 \Theta + \frac{3}{2} (\alpha_1 + \alpha_2) (T - \Theta) + \frac{\gamma_1}{2} (T_w - \Theta)\,, \quad (17)$$

$$\frac{\partial T}{\partial t} = 3(\alpha_3 + \alpha_4)(\Theta - T) + \frac{1}{\rho_{\rm c} c_{\rm c}} \Pi(x, y, t)\,, \quad (18)$$

$$\frac{\partial T_w}{\partial t} = \gamma_2 (\Theta - T_w) - \frac{1}{\rho_{\rm w} c_{\rm w}} Q(x, y, t)\,, \quad (19)$$

where k is the effective heat transfer coefficient,

$$R = \frac{2\Delta x(\sqrt{3}\Delta x - 3l)}{\sqrt{3}\Delta x^2 - \frac{9\sqrt{3}}{4} l^2}\,, \quad (20)$$

and Θ, T, and T_w are functions of (x, y, t). These equations are supplied with the convective boundary conditions:

$$k_{\rm p} \frac{\partial}{\partial x} \Theta(\pm L_x, y, t) = \lambda(\Theta(\pm L_x, y, t) - T_{\rm air}), \quad (21)$$

$$k_{\rm p} \frac{\partial}{\partial y} \Theta(x, \pm L_y, t) = \lambda(\Theta(x, \pm L_y, t) - T_{\rm air}). \quad (22)$$

Here L_x and L_y are linear dimensions of the pack and λ is the heat transfer coefficient between the pack and the air.

Even though the equations (17)–(22) are PDEs, they are considerable simplifications of the full CFD model, offering the advantage that they are tractable for observer, identifier, and control design.

IV. Simulation of the PDE Model

In Figures 8 and 9 we present the result of numerical simulation of the PDE model capturing the thermal runaway effect in a large pack of 215 cells. We use the following model for the Π-term:

$$\Pi_i(t) = \begin{cases} \Pi_{\rm base}, & T_i < T_a \\ \Pi_{\rm burn}, & T_a < T_i < T_b \text{ and } \Pi_i(\tau) > 0 \text{ for } \tau < t \\ 0, & \text{otherwise} \end{cases}$$

for $i = 1, \ldots, N$, where N is the number of cells, T_a is the temperature that triggers heat generation in a cell, T_b is the temperature at which the cell "dies," $\Pi_{\rm base}$ is the normal heat generation in the cells (per unit volume), and $\Pi_{\rm burn}$ is the heat generation per unit volume after the cell is shorted.

In this simulation $T_a = 300K$, $T_b = 450K$, $\Pi_{\rm base} = 0$, and $\Pi_{\rm burn} = 15000000$ W/m^3. Initially, temperature of all the cells is 295K and $\Pi_i(t) = \Pi_{\rm base}$ in all the cells except for one cell, where it is equal to $\Pi_{\rm burn}$. We use the Crank-Nicolson scheme for finite-difference discretization and a modified Thomas algorithm for solving algebraic equations.

In Figure 10 one can see the comparison between the PDE model and the reduced model for one of the cells in the battery pack. The temperature evolution is reasonably well matched and computational savings are huge: the PDE model is about 150 times faster than the reduced model (which is in turn much faster than the CFD model). In order to better fit the reduced model, one would have to tune the independent parameters α_1, α_2, k, and γ_1 using the extremum seeking approach [12].

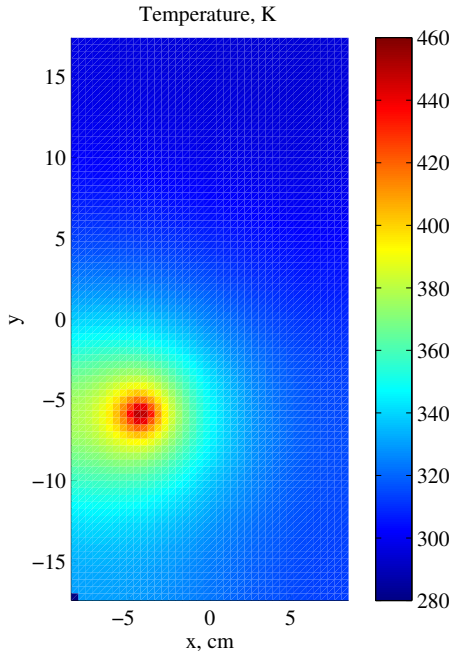

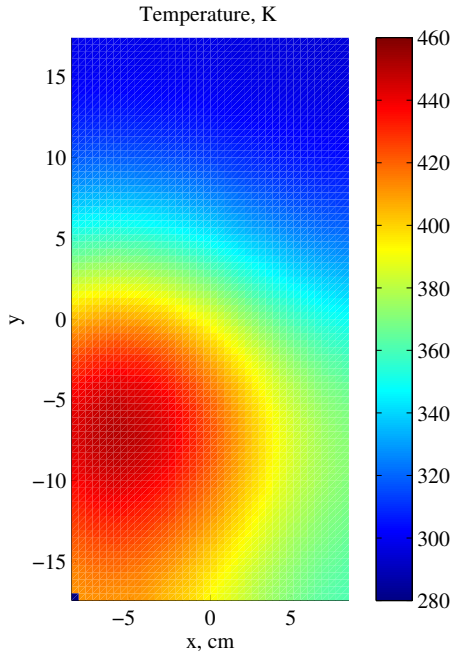

Fig. 8. Temperature distribution in the pack $\Theta(x, y, t)$ at $t = 60$ (left) and $t = 130$ (right).

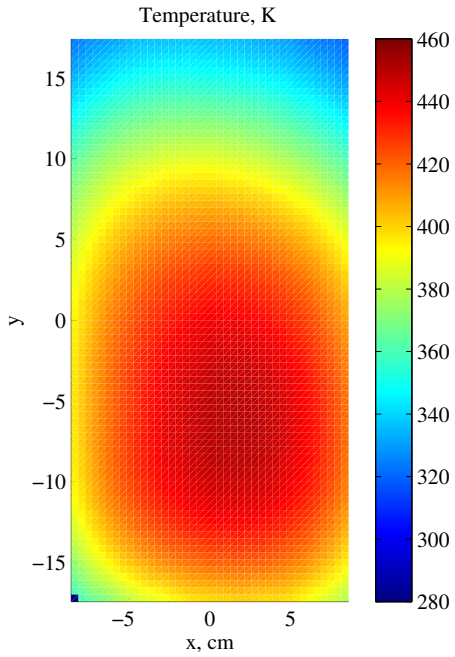

Fig. 9. Temperature distribution in the pack $\Theta(x, y, t)$ at $t = 180$.

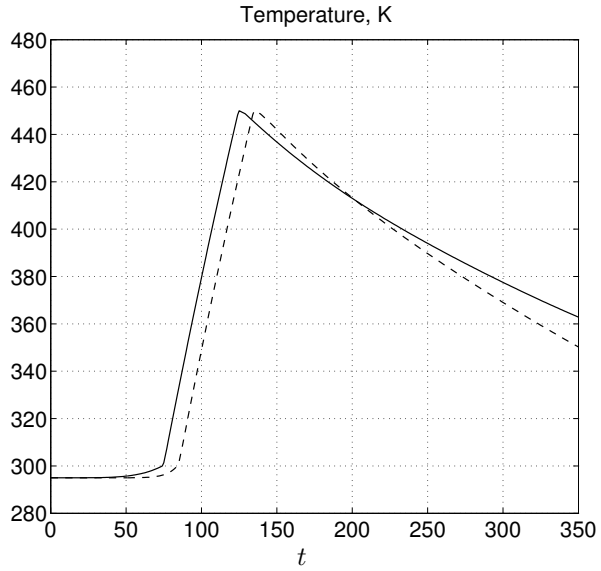

Fig. 10. Temperature evolution of one of the cells (solid—reduced model, dashed—PDE model).

REFERENCES

[1] J.-M. Tarascon and M. Armand, "Issues and challenges facing rechargeable lithium batteries," *Nature*, vol. 414, pp. 359–367, 2001.

[2] M. Armand and J.-M. Tarascon, "Building better batteries," *Nature*, vol. 451, pp. 652–657, 2008.

[3] K. Thomas, J. Newman, and R. Darling, *Mathematical modeling of lithium batteries*, Kluwer Academic/Plenum Publishers, pp. 345–392, 2002.

[4] F. Puglia, S. Cohen, J. Hall, V. Yevoli, "Very large Litium ion cell and battery designs," *5th International Advanced Automotive Battery and Ultracapacitor Conference*, Honolulu, Hawaii, June 2005.

[5] `http://www.teslamotors.com/display_data/TeslaRoadsterBatterySystem.pdf`

[6] `http://www.engadget.com/2006/08/06/another-powerbook-violently-explodes/`

[7] `http://www.dmzhawaii.org/?p=2941`

[8] R. Gitzendanner, F. Puglia, C. Martin, D. Carmen, E. Jones, S. Eaves, "High power and high energy lithium-ion batteries for under-water applications," *Journal of Power Sources*, vol. 136, pp. 416–418, 2004.

[9] R. Gitzendanner, F. Puglia, K. Johanessen, J. Dufrat, "Real world Lithium-ion battery applications—From sub-sea depths to Mars," AIAA paper 2005-5736, *3rd International Energy Conversion Engineering Conference*, San Francisco, California, August 2005.

[10] M. Krstic and A. Smyshlyaev, *Boundary Control of PDEs: A Course on Backstepping Designs*, SIAM, 2008.

[11] A. Smyshlyaev and M. Krstic, *Adaptive Control of Parabolic PDEs*, Princeton University Press, 2010.

[12] K. Ariyur and M. Krstic, *Real Time Optimization by Extremum Seeking Control*, Wiley, 2003.